Derivation of Seasonal Cloud Properties at ARM-NSA from Multispectral MODIS Data

D. A. Spangenberg
Analytical Services and Materials, Inc.
Hampton, Virginia

P. Minnis
National Aeronautics and Space Administration
Langley Research Center
Hampton, Virginia

T. Uttal
National Oceanic and Atmospheric Administration
Environmental Technology Laboratory
Boulder, Colorado

Q. Z. Trepte and S. S.-Mack
Science Applications International Corporation
Hampton, Virginia

Introduction

Improving climate model predictions over earth's Polar Regions requires a complete knowledge of polar cloud microphysics. Over the Arctic, there is minimal contrast between the clouds and background snow surface observed in satellite data, especially for visible wavelengths. This makes it difficult to identify clouds and retrieve cloud properties from space. Variable snow and ice cover, temperature inversions, and the predominance of mixed-phase clouds further complicate cloud property identification. For this study, a solar-infrared infrared near-infrared technique (SINT) first used by Platnick et al. (2001) and a visible-infrared solar-infrared split-window technique (VISST) developed by Minnis et al. (1995) are used to retrieve cloud properties over the Atmospheric Radiation Measurement (ARM) North Slope of Alaska (NSA) Barrow site. Because of the large uncertainty in VISST optical depth τ retrievals using the 0.65-μm channel over bright, highly variable scenes, SINT is used instead. In the SINT algorithm, more accurate optical depths can be achieved using the 1.6-μm channel instead of the 0.65-μm channel due to the relatively dark background surface reflectance and lower sensitivity of τ with reflectance at 1.6 μm.

In this paper, the operational Clouds and the Earth's Radiant Energy System (CERES) cloud mask (Trepte et al. 2002) is first used to discriminate clouds from the background surface in *Terra* Moderate Resolution Imaging Spectroradiometer (MODIS) data. For those pixels tagged as being cloudy, either SINT or VISST is run to obtain both cloud macro and microphysical properties including τ, particle

phase (PP), effective ice crystal diameter D_e, ice water path (IWP), effective liquid drop radius (R_e), liquid water path (LWP), and effective cloud height Z_{eff}. Minnis et al. (2003) give more information on the *Terra*-MODIS cloud property retrievals. The CERES-derived MODIS cloud amounts are validated using the cloud mask from the ARM-NSA micropulse lidar (MPL) based in Barrow. The cloud property retrievals from MODIS are evaluated by comparing them with retrievals obtained from the millimeter-wave cloud radar (MMCR) with additional data coming from the microwave radiometer (MWR) and atmospheric emitted radiance interferometer (AERI) for some of the radar retrieval techniques. All three instruments are based at the ARM-NSA Barrow site.

Satellite Data and Methodology

Terra MODIS 1-km near-infrared (1.6 μm), solar-infrared (3.7 μm), infrared (11 μm, T11), and split-window (12 μm) bands are used as input to the SINT algorithm to determine Arctic cloud properties over snow and ice scenes. Similarly, VISST is run for those scenes where snow and ice are absent with the near-infrared band replaced with the visible 0.65 μm reflectance. The retrievals presented here are from daytime *Terra* overpasses at 1300 and 2000 local time (LT) passing over Barrow between March 2000 and June 2002. Snow and ice maps from the National Snow and Ice Data Center were used to determine whether to run SINT or VISST. The effective cloud height was determined from τ, T11, and atmospheric temperature profiles from the Goddard Earth Observing System Version 4 (GEOS-4) global climate system model. Before comparing MODIS retrievals with those from the ground-based sensors, the satellite data were sub-sampled to 4-km then averaged over a 20-km radius circular region centered on Barrow. Figure 1 shows the geographic area surrounding Barrow used to obtain the spatial average of the MODIS retrievals. Note that much of this area lies over the Arctic Ocean. The 1-minute and 45-m MMCR retrievals were averaged in terms of height, then over a 20-minute time window centered at the *Terra* overpass times.

Results

Prior to obtaining the cloud macro and microphysical properties, the operational CERES cloud detection algorithm, or mask, was used to discriminate clouds from the background snow and ice surface. Figure 2 shows the monthly-mean cloud amount (Ac) from CERES compared to the MPL cloud amount. The plot starts in March and ends in October since only sunlit scenes are considered where the solar zenith angle (SZA) is less than 82°. During this 2-year time frame from March 2000-April 2002, a total of 369 Terra overpasses were used. The lidar is more sensitive to all cloud types, and can be expected to have somewhat higher values, as seen in the figure. Agreement is best in late summer and autumn months, when lidar cloud amounts are near 90% with CERES-MODIS underestimating the actual Ac by no more than 10%. However, during the spring months, CERES values fall short of their MPL counterparts by 20%-30%. This underestimate likely occurred because of the low sun conditions and frequent occurrence of hard-to-detect cirrus clouds over the cold snow and ice surface. The value of the 3.7-μm channel for cloud detection is diminished at large SZAs. The root-mean-squared (rms) difference between CERES and MPL is at a maximum of near 40% in March and April and bottoms out to just under 10% in August.

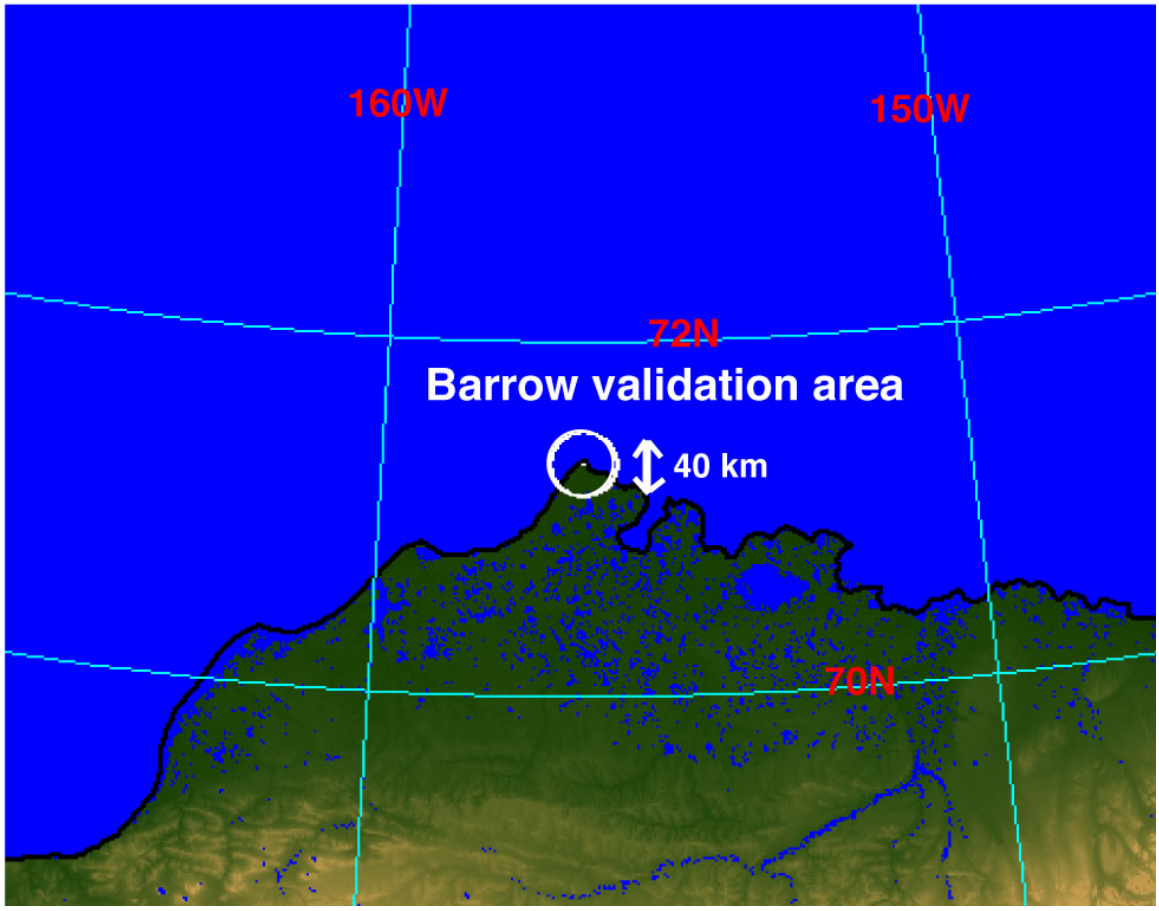

Figure 1. The geographic area surrounding Barrow used to validate the satellite retrievals.

CERES-MODIS cloud properties were retrieved from SINT and VISST during the March 2000-June 2002 time frame. For cloudy pixels within 20 km of Barrow, the cloud properties were averaged and compared to a similar set of retrievals derived using a combination of the ground-based MMCR, MWR, and AERI measurements. Due to the requirement that both satellite and ground-based sensors must both report clouds, and because of the abundance of missing MMCR data, there was an average of 25 comparisons for any given month. Different radar techniques are used to retrieve cloud properties for ice (Matrosov 1999; Matrosov et al. 2002) and liquid (Frisch et al. 1995) cloud phases. These techniques are summarized in Table 1. Each method is listed along with a brief description of the equations used to obtain the cloud properties. Since the radar-microwave radiometer-AERI (combined) retrievals are performed for less than 10% of the Terra overpasses, emphasis will be placed on the MMCR empirical, or regression, methods. Shupe et al. (2001) provide more information on the different radar techniques used to obtain the water contents and particle sizes.

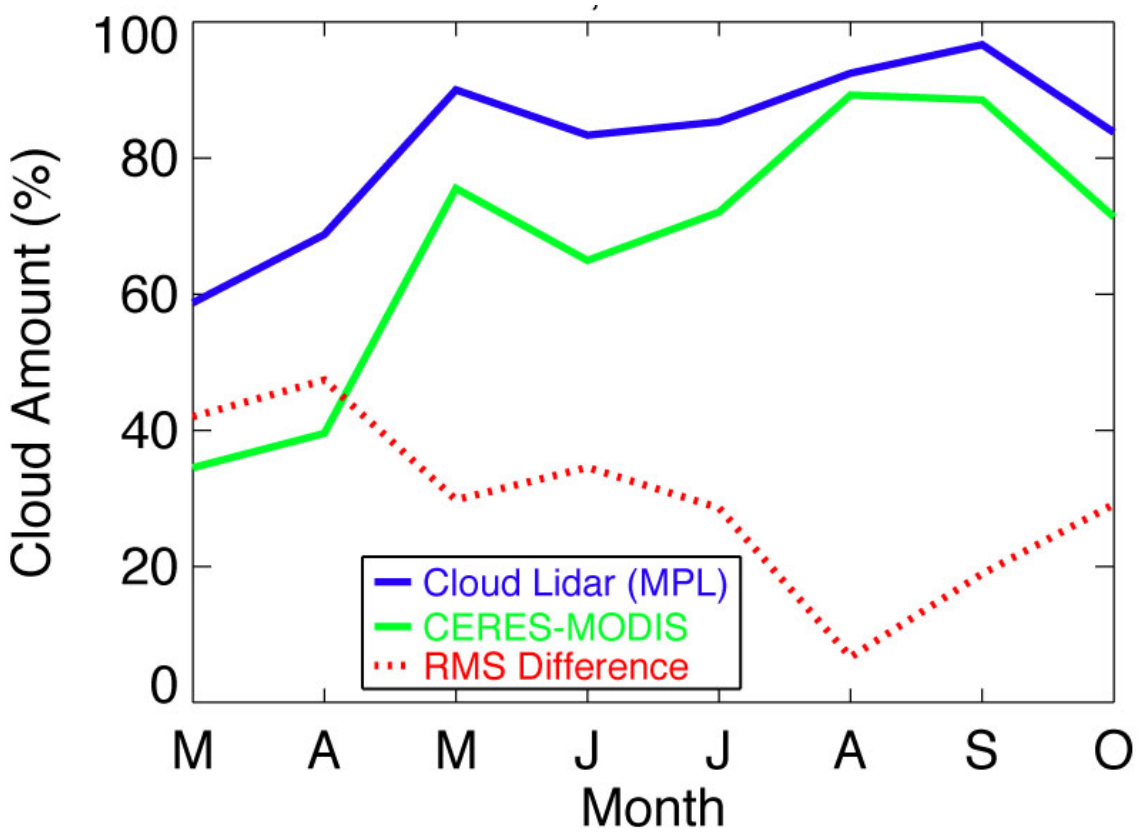

Figure 2. March 2000-April 2002 monthly-mean cloud amounts and RMS difference between Terra-MODIS and MPL over the ARM-NSA Barrow site.

The dominant MMCR cloud phase was found to be mixed and it occurred 40%-60 % of the time period studied (Figure 3). Only during March was the mixed-phase significantly less frequent than the ice phase. The dominant PP in the satellite retrievals was liquid in all months except March and October. Since the satellite cloud property retrieval techniques currently do not have the capability to identify mixed-phase clouds, the liquid phase would be expected instead; liquid drops tend to be found at the top of mixed-phase Arctic clouds (Rangno and Hobbs 2001). Because of the predominance of mixed-phase clouds during the comparison study, MMCR mixed-phase cloud heights are compared to MODIS liquid cloud heights (Figure 4). Since the satellite Z_{eff} is expected to lie between the physical cloud center, or middle, and cloud top, the MMCR cloud top and cloud center are both compared to the MODIS-derived Z_{eff}. In all months, good agreement is seen with the MODIS Z_{eff} lying between the two MMCR curves. The rms difference is lowest for the middle of the MMCR cloud, with values near 1 km. The mean effective cloud heights for liquid (and mixed-phase) clouds are at a minimum in spring, with a value of 0.5 km in April, and then Z_{eff} increases to a maximum of 2.4 km in July.

Table 1. Summary of MMCR Cloud Retrieval Techniques. The ice phase methods are shown in (a) and the liquid methods are in (b). IWC refers to the ice water content, Dm is the mean particle diameter, LWC is the liquid water content, and Z is the radar reflectivity.

(a) MMCR Ice Method	**Description**
radar-microwave radiometer-AERI (rad-mwr-AERI) Matrosov (1999)	IWC = a*Zb ; IWP=Σ(IWC)*dz Dm = 40.5*(Z/IWC)0.53 a = from AERI BT; b scaled linearly through the cloud τ = IWP*(0.021+1.27/Dm)
Regression/Empirical	IWC = a*Zb ; IWP=Σ(IWC)*dz Dm = 40.5*a-0.53 *Z((0.53(1-b)) a = from rad-mwr-AERI method; b=0.63 τ = IWP*(0.021+1.27/Dm)
Doppler Matrosov et al. (2002)	IWC = 1100*Z/(Dm1.9); IWP=Σ(IWC)*dz Dm: Particle-size, fall velocity relationships τ = IWP*(0.021+1.27/Dm)
(b) MMCR Liquid Method	**Description**
radar-microwave radiometer (rad-mwr) Frisch (1995)	LWP: Directly from the microwave radiometer. Re,τ: Microwave radiometer LWP is scaled by radar Z profiles to distribute liquid water content in the clouds. τ = LWP*(0.029+1.3/Re)
Regression/Empirical Fixed-N Variable-N	LWC = (π/6)*e-0.432*N0.5*Z0.5 ; LWP=Σ(LWC)*dz Re = 50* e-0.048*N-0.166*Z0.166 N = 75 cm^{-3} N = N(Z) determined from aircraft measurements τ = LWP*(0.029+1.3/Re)

Comparisons between CERES-MODIS and MMCR ice optical depths are shown in Figure 5. The normalized frequency distribution in Figure 5a shows that both retrievals follow the same trend, with the radar retrievals showing a greater percentage of clouds having ice optical depths under 2. MMCR retrievals are almost identical for the two different regression methods used. The corresponding monthly-mean and rms difference is shown in Figure 5b. For each monthly-mean, the CERES-MODIS τ value is larger than the corresponding one derived from MMCR. The good agreement with rms differences under 3 during March and April likely occurred because there were uniform ice clouds present. During the other 6 months, there was an abundance of multi-layer clouds having different phases. Another source of error is the coastal location of Barrow and the incomplete snow and ice maps at the coastline. This would have led to some overestimation in τ if VISST was run instead of SINT over partially snow and ice covered areas thought to be dark at 0.65 μm. The liquid-phase optical depths are shown in Figure 6. The τ frequency in Figure 6a shows a spike near 5 with reasonably good agreement between the CERES-MODIS and ground-based retrievals. Monthly means from May-September are shown in Figure 6b. For most months, the MODIS curves lie in between the surface-based ones, although the satellite values are higher than the radar regression methods by 3 and 4 in the summer and fall months, respectively. Similar to the case for the ice τ, the overestimate in liquid τ would have occurred if the surface was assumed to be completely clear of snow and ice, when, in fact,

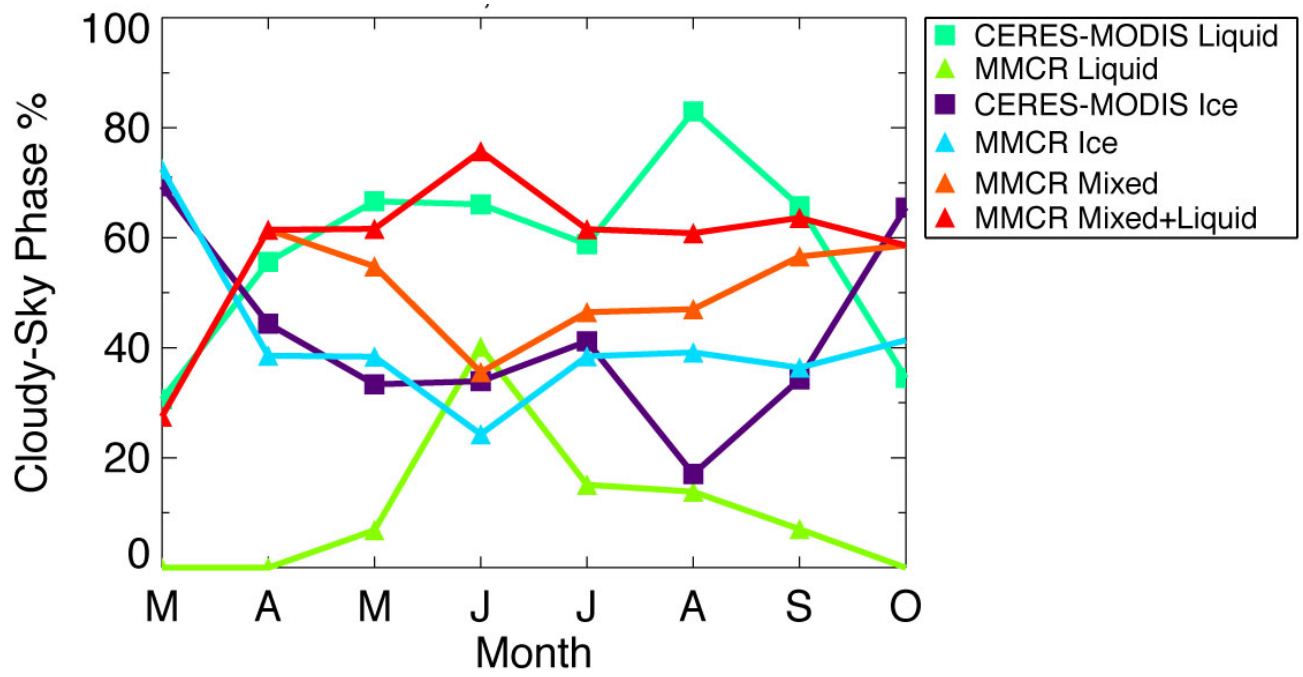

Figure 3. March 2000-June 2002 monthly-mean particle phase reported for Terra-MODIS and MMCR over the ARM-NSA Barrow site.

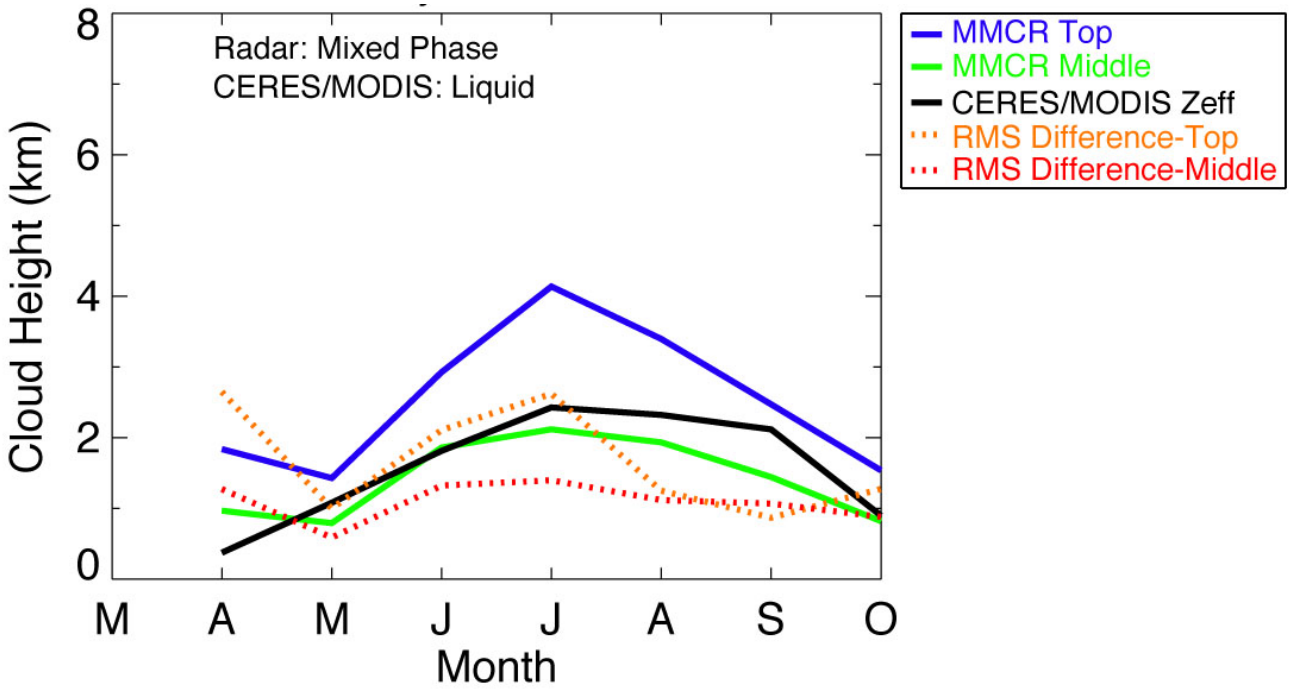

Figure 4. March 2000-June 2002 monthly-mean cloud heights for Terra-MODIS and MMCR retrievals over Barrow. The MMCR depicts the mixed phase whereas the satellite heights are for the liquid phase.

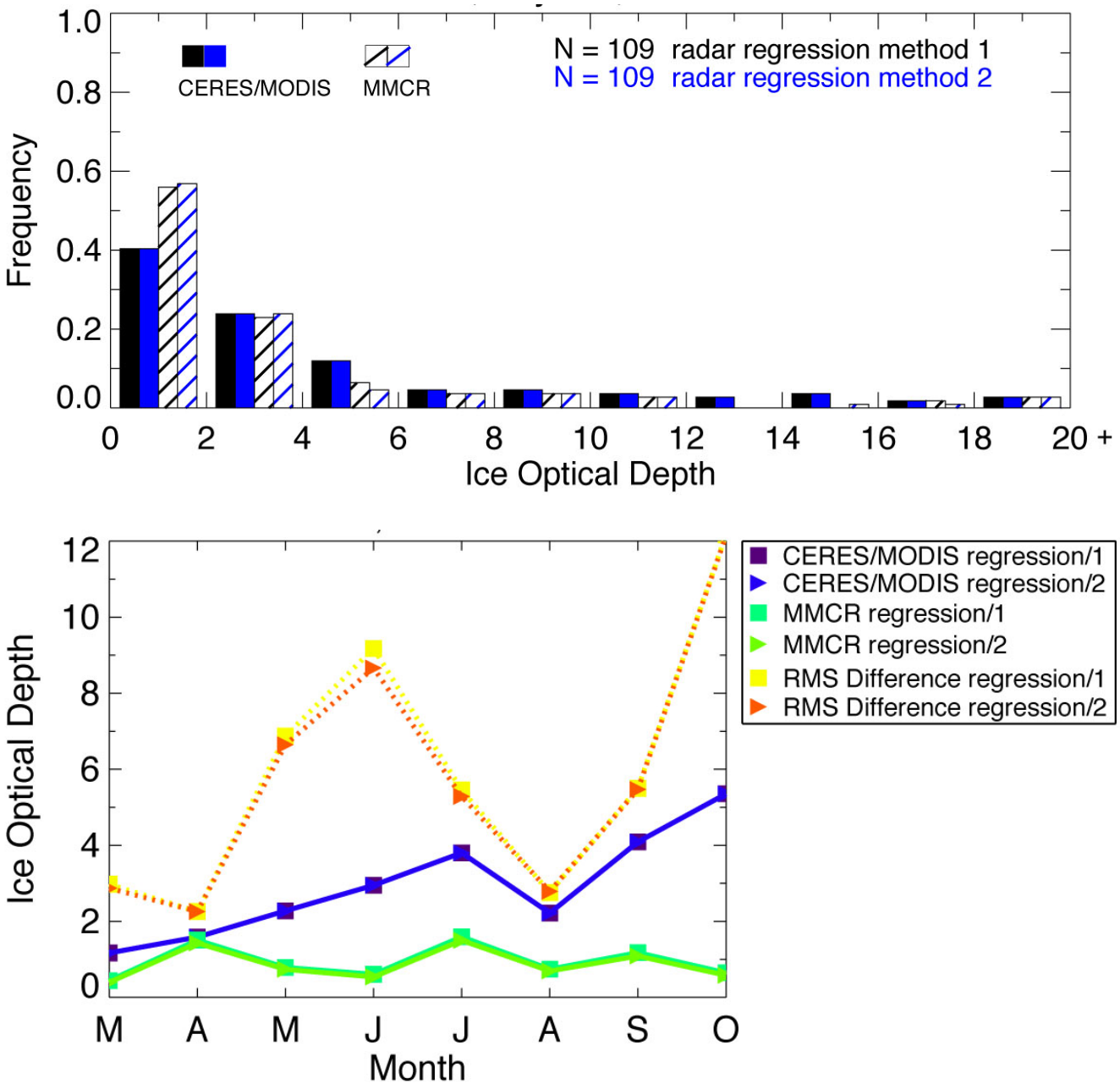

Figure 5. March 2000-June 2002 ice τ for Terra-MODIS and MMCR. The frequency distribution is shown in (a) and the monthly-mean line plots are in (b).

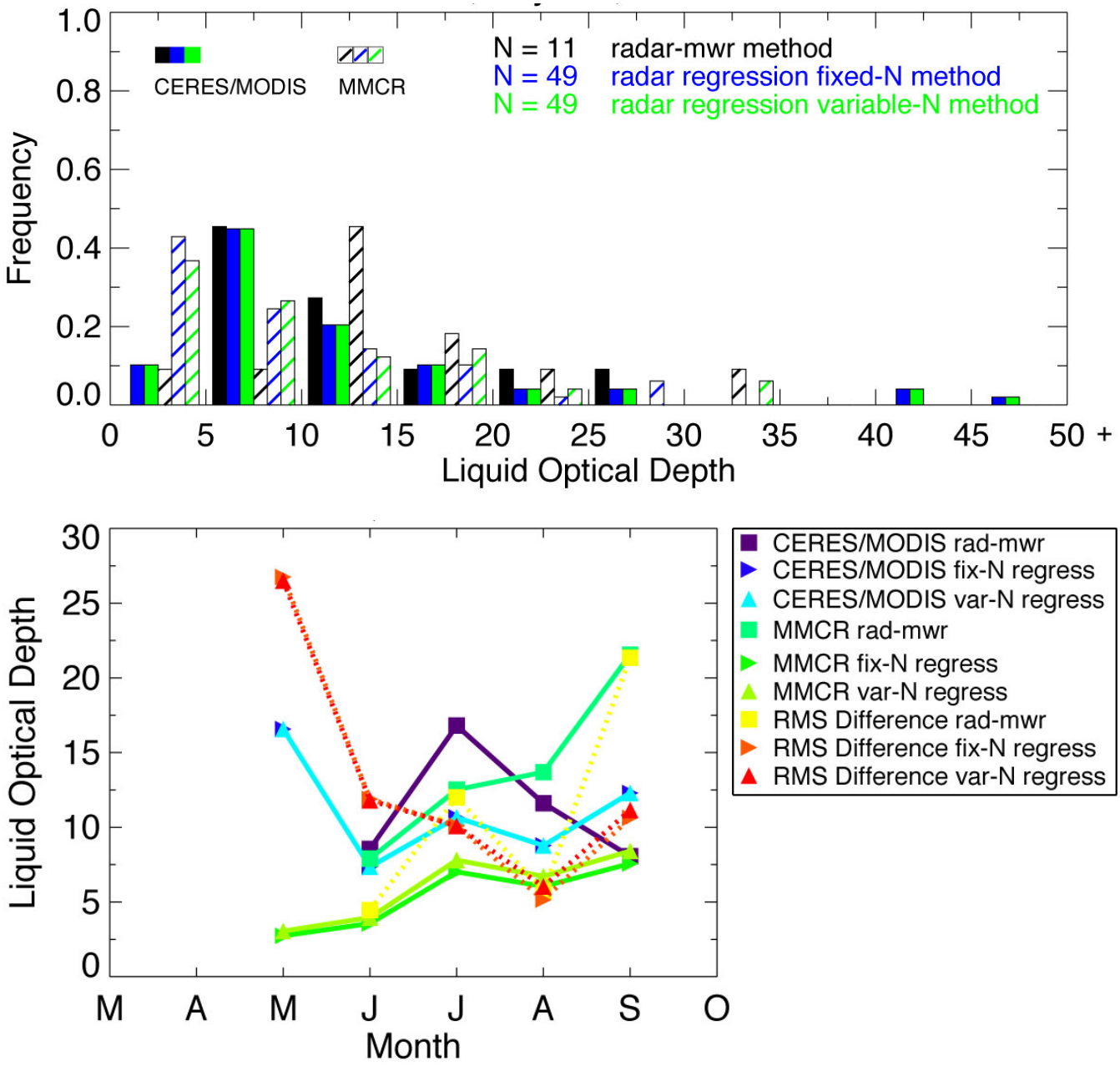

Figure 6. March 2000-June 2002 liquid τ retrievals over Barrow for Terra-MODIS and the ground-based instruments MMCR and MWR. The frequency distribution is shown in (a) and the monthly-mean line plots are in (b).

that was not the case. The large discrepancy in May is likely related to the problem of running VISST for partially snow and ice covered scenes and the lack of liquid clouds cases in that month.

For the effective ice crystal diameter, the MMCR mean diameter (D_m) values were first converted into effective diameters using the equations

$$D_e = 27.5*(D_m)^{0.3}; D_m >= 23.7\ \mu m, \quad (1a)$$

$$D_e = 3.0*D_m; D_m < 23.7\ \mu m. \quad (1b)$$

The results for MMCR and MODIS D_e are presented in Figure 7. The MMCR retrievals start at 90 μm in March, achieve a maximum of 105 μm during the summer months, and then fall back to 90 μm in October. The satellite retrievals fall below the ground-based retrievals in all eight months. Agreement is best in March and October when ice clouds are more prevalent, with D_e values derived from CERES-MODIS falling below the corresponding MMCR regression values by 20 μm. Part of this bias is probably due to differences in definition of the effective diameter used for the satellite and radar retrievals. Conceptually, ice crystal diameters would be expected to follow the MMCR trend of increasing sizes in the warm season as the supply of water vapor increases and the crystals grow larger at the expense of the water drops. MODIS is likely seeing overlapping and mixed-phase cloud structures with the mean signature in the 3.7 μm band pointing towards small ice crystals and increasing the R_e values when thin cirrus clouds overlie liquid (or mixed) PP clouds with the retrieved PP being liquid. The effective liquid drop radii in Figure 8 show the ground-based MMCR retrievals between 4 μm and 8 μm, while their CERES-MODIS counterparts fall between 10 and 16 μm. The rms differences have the same magnitude as the R_e values themselves. While larger CERES-MODIS drops are not inconsistent with similar retrievals of R_e in Arctic clouds by Dong et al. (2001), in-cloud measurements are needed to determine which retrieval is more accurate. Additionally, multilayered ice-over-water clouds need to be screened out of the comparison dataset to determine how those clouds affect the results.

Seasonal statistics were obtained over the Barrow validation area from March 2000 to June 2002. The results are presented in Table 2. Because of the higher number of valid data points and better agreement with the satellite retrievals, the MMCR regression (or empirical) methods were used in the statistical summary. Due to the lack of liquid-only clouds in the spring months, the τ–liquid, R_e, and LWP statistics are not reported in the table for that season. Examining Ac, values from the satellite and surface are highest in fall with values of 82% and 92 %, respectively, with an rms difference of 23%. Spring and summer cloud amounts are 72% and 85% from the MPL, with the CERES cloud mask underestimating Ac by 23% in spring and 14% in summer. During all three seasons, comparing Z_{eff} to the radar middle cloud height yielded better agreement than for the radar tops, with the MODIS retrievals underestimating the surface-derived values by 1.2, 0.6, and 0.3 km in the spring, summer, and fall, respectively. The rms differences ranged from 1.8 km in the fall to 2.2 km in the spring. Optical depths, both liquid and ice, are consistently higher for the MODIS retrievals with the best agreement occurring in the summer for liquid and in spring for ice. The MODIS τ values are 8.7 and 1.7 for these two cases, respectively, with satellite biases of 3.1 for the liquid and 1.0 for the ice. The effective ice diameters are consistently underestimated by MODIS compared to MMCR, with the best agreement

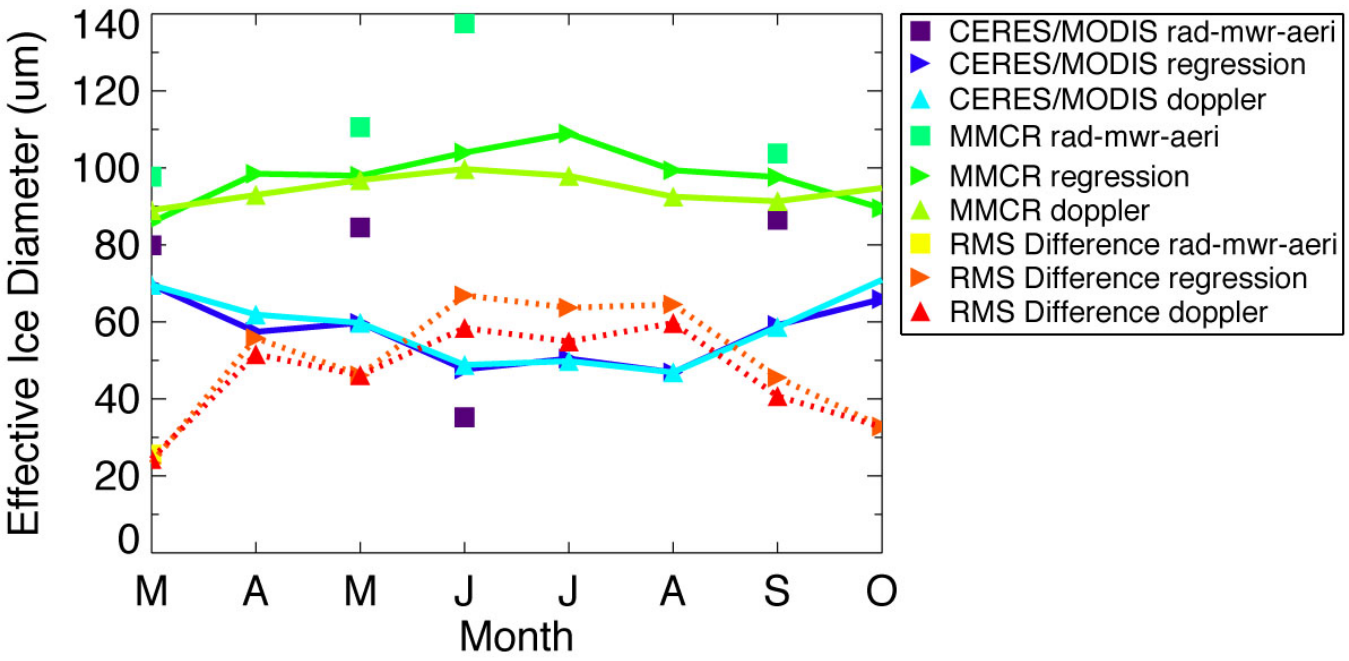

Figure 7. March 2000-June 2002 monthly-mean D_e retrievals over Barrow for Terra-MODIS and the ground-based instruments MMCR, MWR, and AERI.

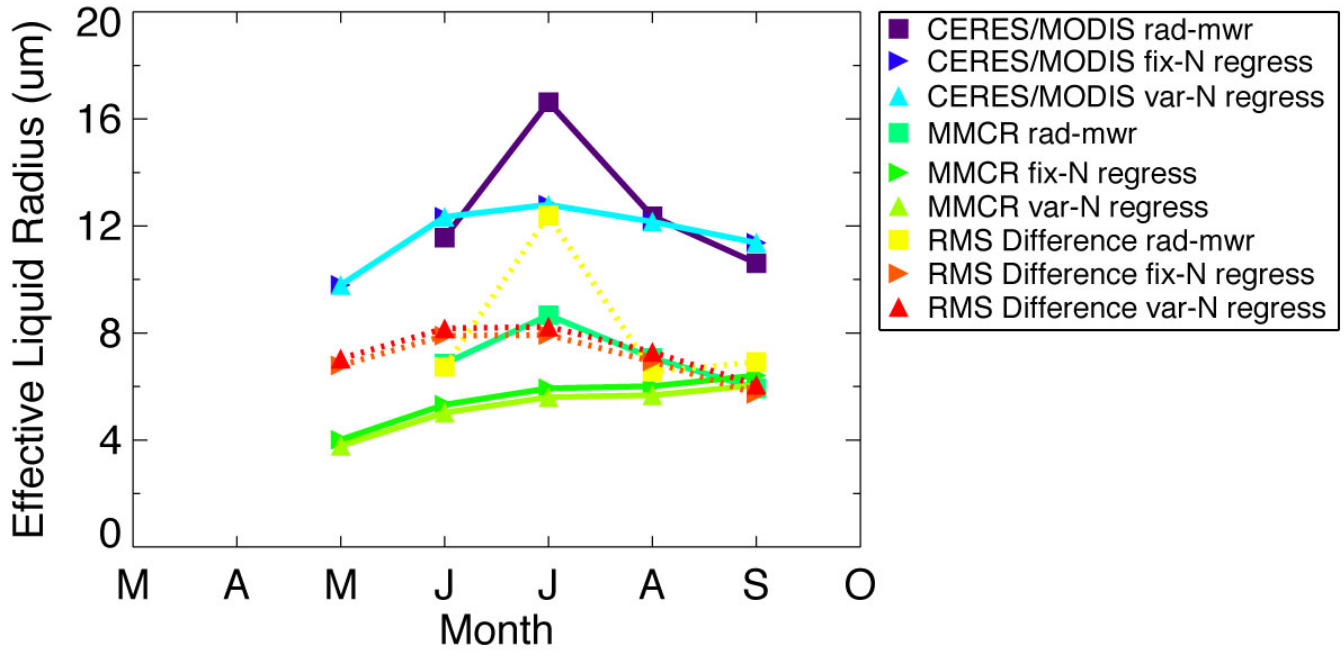

Figure 8. March 2000-June 2002 monthly-mean R_e retrievals over Barrow for Terra-MODIS and the ground-based instruments MMCR, MWR.

Table 2. Seasonal MODIS and MMCR cloud property retrieval statistics for the time frame March 2000-June 2002. Sp = MAM, Su = JJA, and Fa = SO. The last column shows the particular radar method used to obtain the statistics.

Cloud Property	Satellite			Surface			Bias (Sat-Sfc)			RMS Diff			N			Surface Method
	Sp	Su	Fa	Sp	Su	Fa	Sp	Su	Fa	Sp	Su	Fa	Sp	Su	Fa	(M=MMCR)
Ac (%)	50	71	82	72	85	92	-23	-14	-10	40	30	23	171	140	78	MPL
Zeff/Top (km)	1.5	2.5	2.2	4.8	5.6	4.6	-3.3	-3.1	-2.4	4.3	4.2	3.5	67	97	63	M-Top
Zeff/Middle (km)	1.5	2.5	2.2	2.8	3.2	2.5	-1.2	-.6	-.3	2.2	1.9	1.8	67	97	63	M-Middle
τ-Liquid		8.7	12.3		5.6	8.4		3.1	3.9		9.9	11.2		35	10	M-VarN Regress
τ-Ice	1.7	3.3	4.7	0.7	1.1	0.9	1.0	2.2	3.8	4.9	6.5	9.4	34	38	37	M-Regress/1
De (μm)	63	49	63	93	106	93	-30	-57	-31	40	63	39	34	38	37	M-Regress
IWP (gm-2)	51	59	132	86	126	96	-35	-67	37	185	173	169	34	37	36	M-Regress
Re (μm)		12.5	11.4		5.4	6.1		7.1	5.3		7.8	6.1		35	10	M-VarN Regress
LWP (gm-2)		84	93		51	67		33	26		72	71		35	10	M-VarN Regress

occurring in spring and fall when the values are 63 μm for MODIS and 93 μm for MMCR. Again, differences in definitions must be reconciled before drawing any conclusions about the size differences. For those 35 cases having liquid drops during summertime, MODIS retrieved a mean R_e of 12.5 μm whereas MMCR retrieved 5.4 μm, with an rms difference of 7.8 μm. For the IWP, MODIS values are 51, 59, and 132 gm^{-2} in the spring, summer, and fall, respectively. These values are 35 gm^{-2} lower in the spring, 67 gm^{-2} lower in the summer, and 37 gm^{-2} higher in the fall compared to the MMCR retrievals. The rms differences are quite large, with values exceeding the means for each season. The MMCR retrieval methods produced some anomalously high IWP values as the data were not filtered, and this contributed to the large rms differences. Considering the LWP, satellite-retrieved values are 84 gm^{-2} in spring and 93 gm^{-2} in fall. These seasonal mean values exceed their MMCR counterparts by 33 m^{-2} and 26 gm^{-2}.

Conclusions and Future Work

The CERES polar cloud-detection algorithm applied to *Terra*-MODIS data was able to capture most clouds seen in the MPL during the summer and fall seasons, with cloud amounts of 71% and 82 %, respectively. However, because of the presence of low sun and optically-thin cirrus clouds, the springtime cloud amount was 50%, a 23% underestimate. Using *Terra*-MODIS data, the SINT and VISST techniques were able to retrieve realistic cloud macro and microphysical properties over the ARM-NSA Barrow site for sunlit conditions. Ranges in the mean satellite cloud properties retrieved from March 2000-June 2002 for the ice phase include: D_e/49-63 μm, IWP/51-132 gm^{-2}, τ/1.7-4.7, and Z_{eff}/2.7-5.4 km. The corresponding values for liquid are: R_e/11.4-12.5 μm, LWP/84-93 gm^{-2},

τ/8.7-12.3, and Z_{eff}/0.6-0.9 km. The range of the cloud properties represents the differences attributed to the changing seasons. The satellite underestimate in cloud height of up to 0.3-1.2 km, if considering the geometric center of the cloud, was caused by an overestimated optical depth and lack of structure in the vertical temperature profiles.

With respect to PP, MMCR found that mixed-phase clouds are dominant at the NSA Barrow site except for March, when ice alone was the preferred phase. The VISST and SINT satellite retrieval techniques cannot presently discriminate the mixed phase from clouds containing either all ice or all liquid particles. Consequently, the satellite techniques predominantly retrieved liquid PP, which is expected because mixed-phase clouds typically have liquid droplets at their tops. The coastal location of Barrow, along with snow and ice contamination, made it difficult to accurately retrieve the cloud optical depth from space. Consequently, the *Terra*-MODIS optical depths were overestimated by up to 3.8 for ice and 3.9 for liquid. With respect to D_e, the satellite retrievals underestimate their radar-based counterparts by 30-57 μm. This likely occurred because of differences in size definitions and because of the frequent occurrence of multi-layer, mixed-phase clouds making the integrated scene different from that observed in a pristine ice cloud. Finally, R_e values retrieved from the MMCR appear to be small compared the MODIS-retrieved values. To confirm this, in situ aircraft sampling of cloud drop sizes is needed. It should be pointed out here that there are inherent errors in the ground-based MMCR retrievals of 40% for D_e, 75% for IWP, 30% for R_e, and 40% for LWP. These errors likely contribute to some of the discrepancies between MODIS and MMCR cloud property retrievals observed here.

For future work, adjustments will be made to the CERES cloud mask algorithm to capture more clouds during the cold season. Improved snow and ice maps at the coastlines from the National Oceanic and Atmospheric Administration Satellite Services Division can be used to choose whether to run SINT over snow and ice scenes or VISST for open land or ocean. Also, an attempt will be made to resolve the discrepancies between the satellite and surface retrieved particle sizes. Aircraft particle size measurements from the planned Mixed-Phase Arctic Cloud Experiment will be a valuable source of data to continue this study. Finally, an attempt will be made to determine whether it is viable to use MODIS to discriminate mixed-phase scenes from single, uniform cloud decks containing just one phase. To view cloud properties at ARM-NSA and other ARM sites, please see our web page, http://www-pm.larc.nasa.gov.

Acknowledgements

This research was supported by the Environmental Sciences Division of U.S. Department of Energy Interagency Agreement DE-AI02-97ER62341 under the ARM Program. We would like to than Matthew Shupe for providing helpful insights on the analysis and use of the MMCR data.

Corresponding Author

Douglas Spangenberg, d.a.spangenberg@larc.nasa.gov, (757) 827-4647

References

Dong, X., G. G. Mace, P. Minnis, and D. F. Young, 2001: Arctic stratus cloud properties and their effect on the surface radiation budget: Selected cases from FIRE ACE. *J. Geophys. Res*., **106**, D14, 15,297-15,312.

Frisch, A. S., C. W. Fairall, and J. B. Snider, 1995: Measurements of stratus cloud and drizzle parameters in ASTEX with a Ka-band Doppler radar and microwave radiometer. *J. Atmos. Sci*, **52**, 2788-2799.

Matrosov, S. Y., 1999: Retrievals of vertical profiles of ice cloud microphysics from radar and IR measurements using tuned regressions between reflectivity and cloud parameters. *J. Geophys. Res*., **104**, 16,741- 16,753.

Matrosov, S. Y., A. V. Korolev, and A. J. Heymsfield, 2002: Profiling cloud ice mass and particle characteristic size from Doppler radar measurements. *J. Atmos. Ocean. Technol*., **19**, 1003-1018.

Minnis, P., et al., 1995: Cloud Optical Property Retrieval (Subsystem 4.3). In *Clouds and the Earth's Radiant Energy System (CERES) Algorithm Theoretical Basis Document, Vol. III: Cloud Analyses and Radiance Inversions (Subsystem 4).* NASA RP 1376 Vol. 3, edited by CERES Science Team, pp. 135-176.

Minnis, P., D. F. Young, S. Sun-Mack, P. W. Heck, D. R. Doelling, and Q. Z. Trepte, 2003: CERES cloud property retrievals from imagers on TRMM, Terra, and Aqua. *SPIE 10th Intl. Symp. Remote Sens., Conf. on Remote Sens. Clouds and Atmos.*, Barcelona, Spain, September 8-12, pp. 37-48.

Platnick, S. J., Y. Li, M. D. King, H. Gerber, and P. V. Hobbs, 2001: A solar reflectance method for retrieving cloud optical thickness and droplet size over snow and ice surfaces. *J. Geophys. Res*., **106**, D14, 15,185-15,199.

Rangno, A. L., and P. V. Hobbs, 2001: Ice particles in stratiform clouds in the Arctic and possible mechanisms for the production of high ice concentrations. *J. Geophys. Res*., **106**, D14, 15,065-15,075.

Shupe, M. D., T. Uttal, S. Y. Matrosov, and A. S. Frisch, 2001: Cloud water contents and hydrometeor sizes during the FIRE Arctic Clouds Experiment. *J. Geophys. Res*., **106**, D14, 15,015-15,028.

Trepte, Q. Z., P. Minnis, and R. F. Arduini, 2002: Daytime and nighttime polar cloud and snow identification using MODIS data. *Proc. SPIE Conf. on Optical Remote Sens. of the Atmosphere and Clouds III*, Hangzhou, China, October 23-27.